Evaluation of the Catalytic Mechanism of the p21-Activated Protein Kinase PAK2†

Hao Wu,‡ Yi Zheng,§ and Zhi-Xin Wang*,‡

National Laboratory of Biomacromolecules, Center for Molecular Biology, Institute of Biophysics, Academia Sinica, Beijing 100101, People's Republic of China, and Division of Experimental Hematology, Children's Hospital Research Foundation, 3333 Burnet Avenue, Cincinnati, Ohio 45229

Received September 16, 2002; Revised Manuscript Received November 26, 2002

ABSTRACT: The p21-activated kinases (PAKs) play important roles in diverse cellular processes. In the present study, we provide an in-depth kinetic analysis of one of the PAK family members, PAK2, in phosphorylation of a protein substrate, myelin basic protein (MBP), and a synthetic peptide substrate derived from LIM kinase, LIMKtide. Steady-state kinetic analysis of the initial reaction velocity of PAK2 phosphorylation of MBP is consistent with both randomly and compulsorily ordered mechanisms. Further kinetic studies carried out in various concentrations of sucrose revealed that solvent viscosities had no effect on k_{cat}/K_m for either ATP or MBP while k_{cat} was highly sensitive to solvent viscosity, indicating that the enzymatic phosphorylation by PAK2 can be best interpreted by a rapid-equilibrium random bi-bi reaction model, and k_{cat} is partially limited by both phosphoryl group transfer (31 s^{-1}) and the product release (19 s^{-1}). In the phosphorylation of LIMKtide, both k_{cat} and k_{cat}/K_m were insensitive to solvent viscosity, and the product release (86 s^{-1}) was much faster than the phosphoryl group transfer step (19 s^{-1}). These studies suggest that the release of phospho-MBP product is likely partially rate determining for the PAK2-catalyzed reaction since the dissociation rate of products from the PAK2 active site for LIMKtide phosphorylation differs from that of MBP significantly. Such a mechanism is in contrast to the previously established kinetics for the phosphorylation of peptide substrates by cAMP-dependent kinase, in which this process is limited by the release of ADP but not the phospho-peptide product. These results complement previous structure−function studies of PAKs and provide important insight for mechanistic interpretation of the kinase functions.

Protein phosphorylation is one of the major posttranslational modification mechanisms that cells utilize to regulate various signal transduction pathways. The enzymes responsible for catalyzing this reaction are protein kinases. In protein phosphorylation reactions, the terminal (γ) phosphoryl group of ATP is transferred to specific serine and threonine residues by one class of protein kinases and to specific tyrosine residues by another. Protein phosphorylation creates novel recognition motifs for protein−protein interactions, controls protein stability, and regulates enzyme activity. The protein kinases constitute a very diverse set of enzymes. It is predicted that the human genome will encode more than 1000 protein kinases (*1*). Because of their central role in signal transduction, the regulation and function of protein kinases have been the subject of intense interest. Some major insights for cellular signaling have been derived from studies of protein kinases, and certain signaling pathways have been established as cascades of protein kinase reactions.

The p21-activated kinases (PAKs)[1] are members of a family of serine/threonine protein kinases defined by their ability to interact with the small GTPases, Cdc42 and Rac (*2*, *3*). This interaction relieves autoinhibition and stimulates autophosphorylation and activation of PAKs (*4*−*6*). At present, six major members of the PAK family have been identified in mammalian cells, which seem to fall into two categories based on their structures. The first category includes the closely related human PAK1, human PAK2, and mouse PAK3 and the corresponding rat homologues αPAK, γPAK, and βPAK, respectively (*7*−*9*). Recently identified members of the PAK family, PAK4, PAK5, and PAK6, fall into a second category. Like other members of the PAK family, PAKs 4−6 contain an N-terminal regulatory domain and a C-terminal kinase domain. Within the regulatory domain is a GTPase binding domain (GBD) that mediates binding to Cdc42 and Rac. PAK4, PAK5, and PAK6 are highly related to each other but show only about ∼50% identity to the GBD and kinase domains of PAKs 1−3. Outside of the GBD domain and the kinase domain, PAKs 4−6 are entirely different in sequences from PAKs 1−3 (*10*−*12*).

† This work was supported in part by grants from NIH (R03TW01501) and the Ministry of Science and Technology of China (G1999075606).

* To whom correspondence should be addressed. Fax: 86-10-64872026. E-mail: zxwang@sun5.ibp.ac.cn.

‡ Academia Sinica.

§ Children's Hospital Research Foundation.

[1] Abbreviations: PAK, p21-activated protein kinase; GST, glutathione S-transferase; EDTA, ethylenediaminetetraacetic acid; PEP, phospho(enol)pyruvate; LDH, lactate dehydrogenase; PK, pyruvate kinase; MBP, bovine myelin basic protein; MAP, mitogen-activated protein; JNK, jun NH_2-terminal kinase; ERK, extracellular signal-regulated kinase; MEK, MAPK/ERK kinase; LIMKtide, KPDRKKRY**T**VVGNPY; cAPK, cAMP-dependent protein kinase A; SDS−PAGE, sodium dodecyl sulfate polyacrylamide gel electrophoresis.

10.1021/bi026857l CCC: $25.00
Published on Web 01/04/2003

PAKs play an important role in diverse cellular processes, including cytoskeletal dynamics, growth/apoptotic signal transduction, and regulation of transcription factors (*4*−*6*, *13*). Cytoskeletal rearrangements are triggered via phosphorylation of key cytoskeletal associated components by PAKs (*14*). PAK1 phosphorylates and down-regulates myosin light chain kinase activity (*15*) and phosphorylates and activates LIM kinase (*16*). PAK kinase activity has been shown to induce activation of JNK/p38 kinase pathways (*17*−*19*), and a catalytically inactive PAK1 mutant was shown to block JNK/p38 activation in several cell types. Signaling via the ERK MAP kinase pathway is enhanced by phosphorylation of the upstream regulatory kinases Raf and MEK by PAKs (*20*, *21*). PAKs also appear to be involved in apoptosis regulation. For example, constitutively active PAK1 was shown to stimulate Bad phosphorylation; thus, cytochrome *c* release is inhibited, and cell survival is protected by such an effect (*22*−*24*). Additionally, PAK2 is a substrate of caspase and may be cleaved and activated by it (*25*). The activated PAK2 is able to induce some of the morphological and biochemical changes characteristic of programmed cell death (*26*, *27*). PAKs phosphorylate the $p47^{phox}$ component of the phagocyte NADH oxidase in vitro at physiologically relevant sites (*28*), implicating an important regulatory role in the inflammatory response. The involvement of PAK kinase activity in these diverse processes underscores the importance of understanding the molecular basis of PAK functions.

While significant effort has been placed on understanding the structure−function relationship and the mode of regulation of PAKs, little is known about the kinetic processes that occur at the active site of this class of signaling enzymes. A thorough understanding of these processes is germane to informative interpretation of the structure and dynamics of PAKs. In this study, we have employed steady-state kinetic and solvent viscosometric techniques to characterize the catalytic reaction mechanism of PAK2 with respect to its phosphorylation of a protein substrate, myelin basic protein (MBP), and a peptide substrate derived from LIM kinase. Our results indicate that the enzymatic phosphorylation reaction of PAK2 can be best interpreted by a rapid-equilibrium random bi-bi reaction model and that k_{cat} is partially limited by both the phosphoryl group transfer and the product release steps. In addition, our studies also reveal kinetic similarities and differences between PAK2 and other signaling kinases such as ERK2 and cAMP-dependent protein kinase A in terms of their catalytic mechanisms.

EXPERIMENTAL PROCEDURES

Materials. Adenosine 5′-triphosphate (ATP), bovine brain acetone powder, phospho(enol)pyruvate (PEP), nicotinamide adenine dinucleotide, reduced (NADH), lactate dehydrogenase (LDH), pyruvate kinase (PK), urea (ultrapure), and glutathione Sepharose were purchased from Sigma. Sucrose, bovine myelin basic protein (MBP), fetal bovine serum, Grace's insect cell culture medium, and yeastolate solution were purchased from Gibco-BRL. Ficoll 400 and SP Sepharose were purchased from Pharmacia. 3-(*N*-Morpholino)propanesulfonic acid (MOPS) and Tris were purchased from Boehringer Mannheim. Other reagents were local products of analytical grade used without further purification. Double-deionized water was used throughout.

Expression and Purification of Proteins. GST-fusion human PAK2 was generated in a baculovirus system. The full length PAK2 cDNA was cloned into the pVL1392 baculovirus transfer vector together with the cDNA encoding GST, and the recombinant virus was produced by using the BaculoGold kit from Pharmingen. At 2−3 days after infection, cultured Sf9 cells expressing GST-PAK2 were pelleted and resuspended in a lysis buffer containing 50 mM Tris, pH 8.0, 100 mM NaCl, 2 mM EDTA, 0.2% Triton X-100, 10 mM 2-mercaptoethanol, 0.5 mM phenylmethylsulfonyl fluoride (PMSF), 5 μg/mL Aprotinin, 5 μg/mL Leupeptin, 2 mM DTT, and 10% glycerol. The lysate was homogenized and centrifuged at 12 000*g* for 15 min. The supernatant was applied onto a glutathione Sepharose column, and bound GST-PAK2 was eluted with buffer containing 50 mM Tris, pH 8.0, 100 mM NaCl, 2 mM EDTA, 10 mM 2-mercaptoethanol, 10% glycerol, and 10 mM reduced glutathione. The purity of GST-PAK2 was examined by Coomassie Blue staining following SDS−PAGE and was judged at least 95% pure. The enzyme was stored at −70 °C in aliquots. Protein concentrations were determined according to the method of Bradford with bovine serum albumin (BSA) as a standard. If necessary, the GST moiety of the fusions was cleaved by thrombin digestion, followed by incubation with *p*-aminobenzamidine immobilized on agarose beads (Sigma) to remove the thrombin. The constitutively active Cdc42, GST-Cdc42L61, was expressed in *E. coli* and purified according to standard procedures using the affinity matrix Glutathione Sepharose 4B (Amersham Pharmacia Biotech). The protein purity was judged to be over 95% by SDS−PAGE. The purified protein was stored in 20% glycerol at −70 °C. The myelin basic protein (MBP) was isolated from brain acetone powder based on a published protocol (*29*). Protein concentration determination was based on an extinction coefficient calculated from the amino acid composition of bovine MBP, $\epsilon_{280} = 10\,800\ cm^{-1}\ M^{-1}$ (*30*).

Real-Time PAK Kinase Activity Assay. The enzymatic activity of PAK2 was determined with MBP as a substrate using a coupled spectrophotometric assay (*31*). The standard assay for PAK2, except where indicated, was carried out at 25 °C in 1 mL of reaction mixture containing 100 mM MOPS buffer, pH 7.4, 100 mM KCl, 10 mM $MgCl_2$, 200 μM NADH, 1 mM phospho(enol)pyruvate, 20 units/mL lactate dehydrogenase, 15 units/mL pyruvate kinase (buffer A), and different concentrations of substrates. Reactions were initiated by the addition of PAK2 to the reaction mixture. Progress of the reactions was monitored continuously by following the formation of NAD^+ at 340 nm, on a Shimadzu UV2501PC14 spectrophotometer. Initial rates were determined from the linear slope of progress curves obtained with an extinction coefficient for NADH of 6220 $cm^{-1}\ M^{-1}$ at 340 nm. The concentrations of substrates and PAK2 are given in the text or in the figure legends. LIMKtide, a synthetic peptide derived from the PAK phosphorylation site of LIM kinase (residues 500−514, KPDRKKRY**T**VVGNPY), was synthesized using standard protocol, purified by reverse-phase preparative HPLC chromatography, and characterized by MALDI-TOF mass spectrometry by ADI Inc. The concentration of LIMKtide was determined by turnover with the GST-PAK2 under limiting peptide.

Solvent Viscosometric Studies. Steady-state assays were carried out as described above in buffer A containing varied

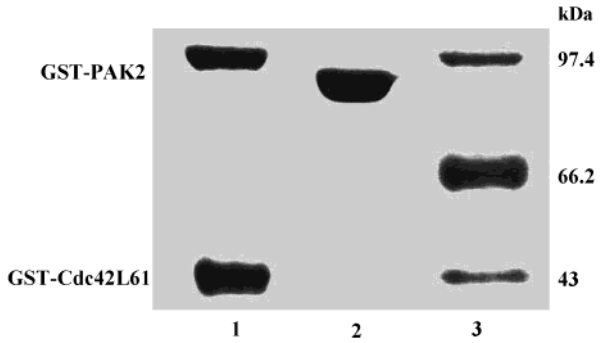

FIGURE 1: SDS−PAGE of unphosphorylated and phosphorylated GST-PAK2. Lane 1, phosphorylated GST-PAK2 and GST-Cdc42L61. Lane 2, unphosphorylated GST-PAK2. Lane 3, molecular mass markers of 97.4, 66.2, and 43 kDa, respectively.

sucrose or Ficoll 400. Relative solvent viscosities (η^{rel}) were determined from the following equation:

$$\eta^{rel} = (t/t^0)(\rho/\rho^0) \quad (1)$$

where η^{rel} is the solvent viscosity relative to the buffer containing no viscosogen, t is the solvent transit time measured by an Ostwald capillary viscometer (*32*), and ρ is the solvent specific gravity (*33*). Superscript 0 indicates conditions of the buffer with no viscosogen. All solvent viscosity measurements were performed in triplicate and did not deviate by more than 2% in values.

RESULTS

Autophosphorylation and Activation of GST-PAK2. Recombinant human PAK2 was expressed in insect cells as a GST-fusion and was purified using affinity chromatography on glutathione-Sepharose. The purified GST-PAK2 was an inactive enzyme and can be activated by autophosphorylation in the presence of constitutively active Rho family small G proteins, Cdc42 or Rac. A comparison of the phosphorylation profile and the kinase activity of γPAK showed that autophosphorylation is through a bipartite mechanism with the regulatory domain autophosphorylated at multiple residues, and the enzymatic activation coincides with autophosphorylation of the catalytic domain at Thr-402 (*34*). In this study, autophosphorylation and activation of GST-PAK2 was carried out in a reaction mixture containing 100 mM MOPS (pH 7.4), 10 mM $MgCl_2$, 2 mM DTT, 1 mM ATP, 15 μM GST-Cdc42L61, and 3 μM GST-PAK2 at 30 °C. At defined time intervals, an aliquot was taken from the reaction mixture and assay for enzyme activity. When GST-PAK2 was examined in our assay system with MBP as a substrate, we observed a maximum activation after 3 min of incubation with 1 mM ATP and 15 μM Cdc42L61. Autophosphorylation of GST-PAK2 was analyzed by SDS−PAGE on a 10% polyacrylamide gel. The autophosphorylation and activation of GST-PAK2 correlated with a major electrophoresis band shift as shown in Figure 1. The GST moiety did not serve as a substrate of PAK2 since it was not phosphorylated under similar conditions (data not shown). Cdc42L61 was removed by gel filtration (Sepharcryl-S100 column, Pharmacia LKB) after PAK2 autophosphorylation, and the active GST-PAK2 preparation was used for further kinetic study.

Steady-State Kinetics of the PAK2-Catalyzed Reaction. To characterize the steady-state kinetic properties of PAK2, we first sought to measure the kinase activity of PAK2 by following ADP formation using an enzyme-coupled spectrophotometric assay. Because PAK2 displays a significant ATPase activity in the absence of any added protein substrate, we were able to obtain the kinetic parameters for the ATP hydrolyzing activity of PAK2 from a catalytic amount of the phosphorylated PAK2. The experimental data fit the Michaelis−Menten equation with a K_m of 150 ± 10 μM and a k_c of 0.26 ± 0.01 s^{-1}.

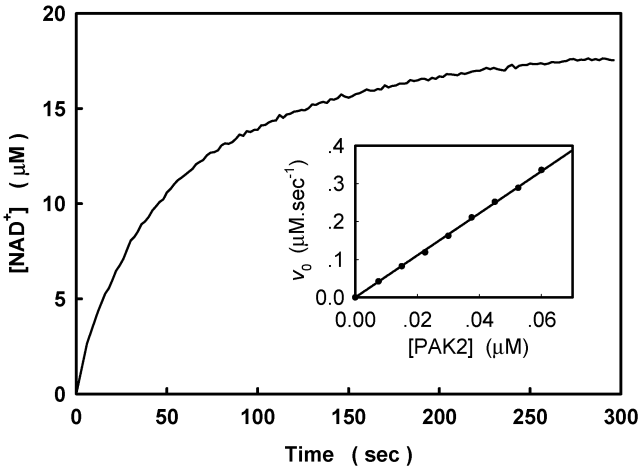

FIGURE 2: Reaction time course of MBP phosphorylation by PAK2. The time-dependent phosphorylation of MBP was monitored by measuring the absorbance changes at 340 nm using a coupled spectrophotometric assay as described in Experimental Procedures. The concentration of PAK2 was 100 nM; the concentration of MBP was 10 μM; and the concentration ATP was 1 mM. Inset: Plot of initial velocity of the PAK2-catalyzed reaction against varying concentrations of enzyme.

To determine the kinetic parameters of PAK2 kinase activity, MBP was used as a protein substrate. Figure 2 shows a reaction time course of the MBP phosphorylation by PAK2. The time-dependent phosphorylation of MBP was monitored by following absorbance changes at 340 nm, and the absorbance units (A_{340}) were converted to the NADH concentration by using the extinction coefficient $\epsilon_{340} = 6.22 \times 10^3$ cm^{-1} M^{-1}. Since the spontaneous ATP hydrolysis by PAK2 occurs in parallel to the phosphorylation reaction, the assays were corrected for the ATPase effect that is taken as the observed absorption changes in the absence of MBP. X-ray crystallographic study has suggested that the PAKs exist as a dimer (*35*). Thus, it would be of interest to know whether the enzyme activity obtained for PAK differs as a function of PAK concentration. The inset of Figure 2 shows that the initial velocity of the PAK2-catalyzed reaction is proportional to the enzyme concentration. The linear relationship between velocity and enzyme concentration suggests that under the conditions used in the present study, either no dimerization occurs in the range of enzyme concentration used, or dimerization could occur without any activity changes. As seen in Figure 2, although the phosphorylation of MBP by PAK2 has been mapped to a single site previously (*36*), the amount of NAD^+ produced exceeded the initial concentration of MBP by 2-fold, suggesting that at least two sites are available for PAK2 modification when a large amount of the substrate is consumed. Therefore, we pursued the kinetic studies using the continuous kinase assay under the conditions in which the initial portion of the reaction profile was linear. The initial rate phase of the

Scheme 1

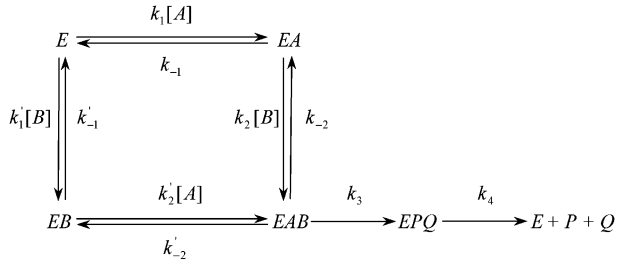

PAK2-catalyzed reaction typically persists for 30−60 s. Additional experiments were carried out with GST-cleaved-PAK2 to see if the GST moiety in GST-PAK2 fusion may affect the kinetics of the reaction. Essentially identical values of k_{cat} and K_m were obtained in the presence of 1 mM ATP, indicating that the GST portion of the fusion does not interfere with the PAK2-catalyzed reaction. Thereafter, we used GST-fused PAK2 for further investigation.

Scheme 1 describes the minimal kinetic mechanism for the phosphorylation of a protein substrate by a protein kinase, where k_3 is the rate constant for the phosphoryl group transfer step, and k_4 is the rate constant for products release, E represents enzyme, and A and B represent ATP and the protein substrate, respectively. The exact steady-state solution for this mechanism could be very complicated. However, as pointed out by Laidler and Bunting (*37*, *38*), the general ternary-complex mechanism may lead to a simple rate equation if one of the following conditions is satisfied:
(1) When there is an equilibrium among the E, EA, and EB species. The rate equation can be simplified by

$$v = \frac{\frac{k_3k_4}{(k_3+k_4)}[\mathrm{E}]_0[\mathrm{A}][\mathrm{B}]}{\frac{(k_{-2}+k'_{-2}+k_3)(k_{-1}k'_{-1}k_4+k_1k'_{-1}k_4[\mathrm{A}]+k'_1k_{-1}k_4[\mathrm{B}])}{(k_3+k_4)(k'_1k_{-1}k'_2+k_1k_2k'_{-1})}+[\mathrm{A}][\mathrm{B}]} \quad (2)$$

(*2*) When the rate of the formation of the ternary complex EAB from one of the binary complexes is negligible as compared with the rate of its formation from the other binary complex. If the ternary complex EAB can be formed from only EA, and B is not allowed to form the complex EB, the steady-state rate equation is given by

$$v = \frac{\frac{k_3k_4}{(k_3+k_4)}[\mathrm{E}]_0[\mathrm{A}][\mathrm{B}]}{\frac{k_{-1}k_4(k_{-2}+k_3)}{k_1k_2(k_3+k_4)}+\frac{k_4(k_{-2}+k_3)}{k_2(k_3+k_4)}[\mathrm{A}]+\frac{k_3k_4}{k_1(k_3+k_4)}[\mathrm{B}]+[\mathrm{A}][\mathrm{B}]} \quad (3)$$

The first condition corresponds to a partial rapid-equilibrium random ternary-complex mechanism, and the second one corresponds to an ordered ternary-complex mechanism. These two mechanisms give rise to the equation of the general form

$$v = \frac{V_{max}[\mathrm{A}][\mathrm{B}]}{K_{iA}K_{mB}+K_{mB}[\mathrm{A}]+K_{mA}[\mathrm{B}]+[\mathrm{A}][\mathrm{B}]} \quad (4)$$

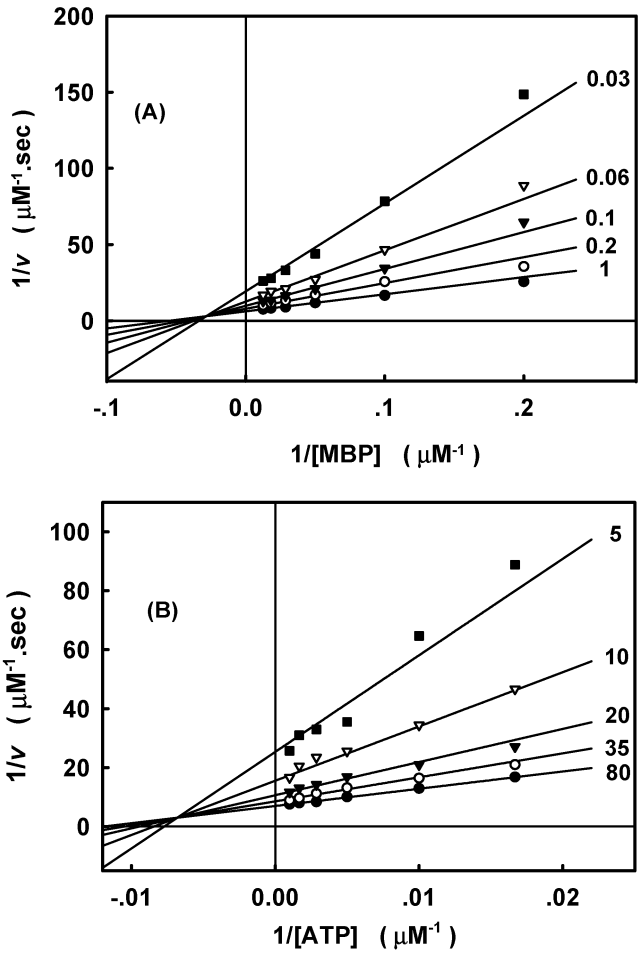

FIGURE 3: Steady-state kinetic analysis of MBP phosphorylation by PAK2. The initial velocities at various concentrations of MBP and ATP were determined by a coupled spectrophotometric assay. (A) Double-reciprocal plots of PAK2 activity versus the MBP concentration at increasing concentrations of ATP (as indicated on the graphs in mM). (B) Double-reciprocal plots of PAK2 activity versus the ATP concentration at increasing concentrations of MBP (as indicated on the graphs in μM). The concentration of PAK2 in the reactions was 15 nM. The Michaelis−Menten model describing two-substrate sequential binding was globally fit to the data by nonlinear regression analysis. The optimized kinetic parameters obtained from the regression analysis are described in Table 1.

If the entire random segment is assumed to be at equilibrium, the final equation is identical to eq 4. In this case, the rate constant compositions of several kinetic constants change.

To define the basic kinetic mechanism of the PAK2-catalyzed reaction, a data set of initial velocities was obtained over a wide range of ATP and MBP concentrations. Figure 3 shows that double reciprocal plots of the initial velocity versus either ATP or MBP concentration are linear and display a pattern of intersecting lines above the abscissa at a common vertical coordinate. This is consistent with both randomly and compulsorily ordered mechanisms. The experimental data were fitted to eq 4, and the kinetic parameters determined are summarized in Table 1.

Effects of Viscosogens on the Steady-State Kinetic Parameters. The kinetic parameters described in eq 4 are a composite of microscopic rate constants combined in a manner dependent upon the order of substrate addition. The steady-state kinetic data obtained for the PAK2-catalyzed reaction could not distinguish between a randomly ordered and a compulsorily ordered mechanism. However, if the

Table 1: Kinetic Constants and Viscosity Effects for Phosphorylation of MBP by PAK2[a]

kinetic parameter	value	method of determination
k_{cat}	$12 \pm 0.3\ s^{-1}$	measured
$K_{m(MBP)}$	$17 \pm 1\ \mu M$	measured
$K_{m(ATP)}$	$71 \pm 7\ \mu M$	measured
$K_{i(ATP)}$	$147 \pm 20\ \mu M$	measured
$(k_{cat})^{\eta}$	0.62 ± 0.02	measured
$(k_{cat}/K_{m(MBP)})^{\eta}$	-0.07 ± 0.01	measured
$(k_{cat}/K_{m(ATP)})^{\eta}$	0.09 ± 0.01	measured
$k_{cat}/K_{m(MBP)}$	$0.68 \pm 0.05\ \mu M^{-1}\ s^{-1}$	$k_{cat}/K_{m(MBP)}$
$k_{cat}/K_{m(ATP)}$	$0.16 \pm 0.02\ \mu M^{-1}\ s^{-1}$	$k_{cat}/K_{m(ATP)}$
$K_{i(MBP)}$	$35 \pm 7\ \mu M$	$K_{i(ATP)}K_{m(MBP)}/K_{m(ATP)}$
$k_{2(MBP)}$	$\geq 7.5 \pm 0.7\ \mu M^{-1}\ s^{-1}$	$(k_{cat}/K_{m(MBP)})(k_{-2(MBP)} + k_3)/k_3$
$k_{-2(MBP)}$	$\geq 306 \pm 11\ s^{-1}$	$k_3(1 - (k_{cat}/K_{m(MBP)})^{\eta})/(k_{cat}/K_{m(MBP)})^{\eta}$
$K'_{2(ATP)}$	$1.9 \pm 0.2\ \mu M^{-1}\ s^{-1}$	$(k_{cat}/K_{m(ATP)})(k'_{-2(ATP)} + k_3)/k_3$
$K'_{-2(ATP)}$	$330 \pm 35\ s^{-1}$	$k_3(1 - (k_{cat}/K_{m(ATP)})^{\eta})/(k_{cat}/K_{m(ATP)})^{\eta}$
k_3	$31 \pm 1\ s^{-1}$	$k_{cat}/(1 - (k_{cat})^{\eta})$
k_4	$19 \pm 1\ s^{-1}$	$k_{cat}/(k_{cat})^{\eta}$

[a] The kinetic parameters were measured in 50 mM MOPS (pH 7.4) buffer at 25 °C using a coupled enzyme assay. [PAK2] = 15 nM, [ATP] = 0.03−1 mM, and [MBP] = 5−80 μM, 10 mM $MgCl_2$. k_{cat}, $K_{m(ATP)}$, $K_{m(MBP)}$, and $K_{i(ATP)}$ were directly measured from the steady-state kinetic analysis. $(k_{cat})^{\eta}$, $(k_{cat}/K_{m(MBP)})^{\eta}$, and $(k_{cat}/K_{m(ATP)})^{\eta}$ are the slope values for plots of the steady-state kinetic parameters as ratios in the absence and presence of sucrose versus the relative solvent viscosities. Negative value of $(k_{cat}/K_{m(MBP)})^{\eta}$ was treated as zero.

kinetic mechanism of PAK2 is ordered, it has to be ordered with ATP binding first since PAK2 displays measurable ATPase activity in the absence of MBP. To analyze the kinetic mechanism further, we next carried out the solvent viscosometric studies of the PAK2-catalyzed reactions. The effect of solvent viscosity on the rate parameters for enzyme-catalyzed reactions has been given a substantial amount of theoretical and experimental consideration (*39*−*42*). For a simple bimolecular process in solution, the association and dissociation constants are inversely proportional to the relative microviscosity of bulk solvent at constant temperature (*39*). Consequently, solvent viscosity studies have been classically used to isolate those processes within an enzymatic reaction pathway that are subject to diffusion control. The minimal kinetic mechanism for the PAK2-catalyzed ATP hydrolysis reaction can be written as

$$A + E \underset{k_{-1}}{\overset{k_1}{\rightleftharpoons}} EA \xrightarrow{k_c} EP \xrightarrow{k_d} E + P$$

By using Cleland's method of net rate constants (*43*), the kinetic parameters, k_{cat} and K_m, are given by

$$k_{cat} = \frac{k_c k_d}{k_c + k_d} \tag{5}$$

and

$$K_m = \frac{k_{-1} + k_c}{k_1}\frac{k_d}{k_c + k_d} \tag{6}$$

Combining eqs 5 and 6, we obtain

$$\frac{k_{cat}}{K_m} = \frac{k_1 k_c}{k_{-1} + k_c} \tag{7}$$

Since k_1, k_{-1}, and k_d are presumed to represent diffusion controlled processes, these rate constants will be dependent on the relative viscosity of the solvent. The relative solution viscosity (η^{rel}) can be equated to the ratio of the microscopic rate constants

$$\eta^{rel} = k_1^0/k_1 = k_{-1}^0/k_{-1} = k_d^0/k_d \tag{8}$$

By taking separately the ratio of eqs 5 and 7 in the absence and presence of viscosogen according to eq 8, two linear equations are derived upon plotting k_{cat}^0/k_{cat} and $(k_{cat}/K_m)^0/(k_{cat}/K_m)$ as a function of η^{rel}. The slopes of these lines are given by

$$(k_{cat})^{\eta} = \frac{k_c}{k_c + k_d^0} \tag{9}$$

and

$$\left(\frac{k_{cat}}{K_m}\right)^{\eta} = \frac{k_c}{k_{-1}^0 + k_c} \tag{10}$$

where k_{-1}^0 and k_d^0 are the dissociation rate constants of substrate and product, respectively, when $\eta^{rel} = 1$. Thus, $(k_{cat})^{\eta}$ and $(k_{cat}/K_m)^{\eta}$ can vary between 0 and 1, the limit of diffusion-control. When the phospho-transfer step is much slower than product release (i.e., $k_c \ll k_d^0$), $(k_{cat})^{\eta}$ approaches the limiting value of zero. Likewise, when the substrate is nonsticky (i.e., $k_c \ll k_{-1}^0$), $(k_{cat}/K_m)^{\eta}$ approaches the limit of zero.

Figure 4 shows the effect of viscosogens on the ATPase activity of PAK2. Both k_{cat} and k_{cat}/K_m appear to be insensitive to the relative solvent viscosity. The lack of a viscosity effect on both k_{cat} and k_{cat}/K_m supports a kinetic scheme in which ATP is in rapid equilibrium with the Michaelis complex, whose breakdown to form the reaction product is entirely limited by the ATP hydrolysis step. In such a model, the true affinity of ATP to form the binary complex is given by its K_m value (i.e., $K_m = k_{-1}/k_1 = 150\ \mu M$). Furthermore, these data suggest that viscosogen has no measurable influence on the structure of the enzyme and the orientation of active-site residues.

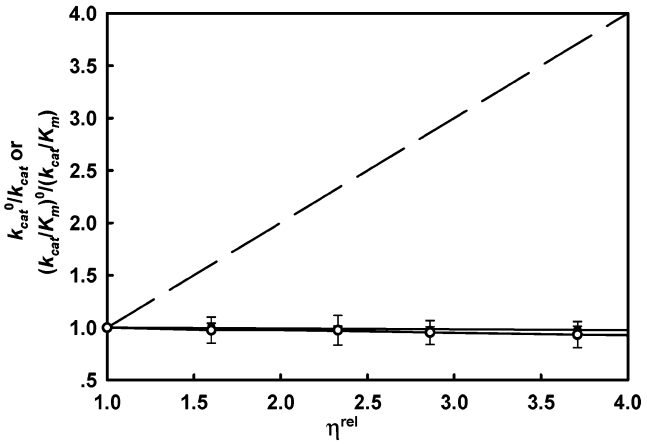

FIGURE 4: Solvent viscosity effects on k_{cat} and k_{cat}/K_m of the ATPase activity of PAK2. Viscosity effects on k_{cat} or k_{cat}/K_m were determined as a function of increasing concentrations of sucrose. k_{cat}^0/k_{cat} (●) and $(k_{cat}/K_m)^0/(k_{cat}/K_m)$ (○) are the ratios of the observed k_{cat} and k_{cat}/K_m values in the absence and presence of viscosogen, respectively. η^{rel} is the relative solvent viscosity. The dashed line has a slope of 1.

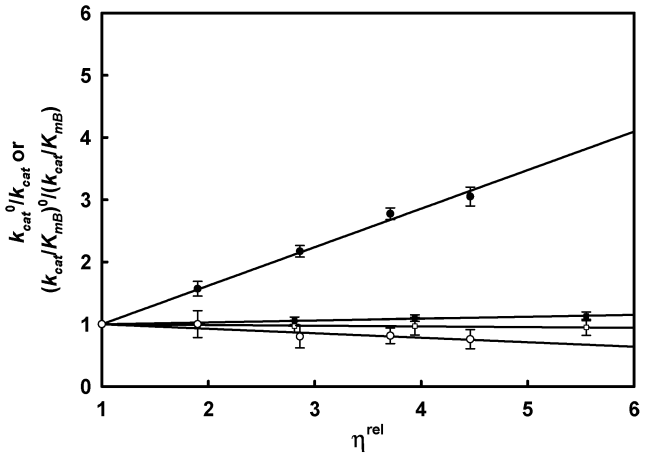

FIGURE 5: Dependence of the steady-state kinetic parameters for the MBP phosphorylation on the relative viscosity of solvent at saturating concentration of ATP. η^{rel} represents the ratio of solution viscosity in the presence of viscosogen (sucrose or Ficoll 400) over that in the absence of viscosogen. k_{cat}^0/k_{cat} and $(k_{cat}/K_{mB})^0/(k_{cat}/K_{mB})$ are the ratios of the observed k_{cat} and k_{cat}/K_{mB} values in the absence and presence of viscosogen, respectively. ATP was at 1 mM with varying MBP concentrations. (●) k_{cat}^0/k_{cat} in the presence of sucrose; (○) $(k_{cat}/K_{mB})^0/(k_{cat}/K_{mB})$ in the presence of sucrose; (■) k_{cat}^0/k_{cat} in the presence of Ficoll 400; (□) $(k_{cat}/K_{mB})^0/(k_{cat}/K_{mB})$ in the presence of Ficoll 400.

Saturating ATP and Varying MBP Concentrations. We next attempted to define the diffusion-controlled steps in the catalytic reaction of PAK2 by examining the steady-state phosphorylation of MBP in the presence of sucrose. Under the condition of saturating ATP concentration (1 mM), the mechanism of PAK2-catalyzed MBP phosphorylation can be written as

$$B + EA \underset{k_{-2}}{\overset{k_2}{\rightleftharpoons}} EAB \xrightarrow{k_3} EPQ \xrightarrow{k_4} E + P + Q$$

In this scheme, the substrate MBP combines with the enzyme−ATP complex to form the active ternary complex by the second-order association rate constant, k_2, and the dissociation rate constant, k_{-2}. The slopes of k_{cat}^0/k_{cat} and $(k_{cat}/K_{mB})^0/(k_{cat}/K_{mB})$ versus η^{rel} are given by

$$(k_{cat})^\eta = \frac{k_3}{k_3 + k_4^0} \tag{11}$$

and

$$\left(\frac{k_{cat}}{K_{mB}}\right)^\eta = \frac{k_3}{k_{-2}^0 + k_3} \tag{12}$$

Figure 5 shows the effect of increasing solvent viscosity on the steady-state kinetic parameters for the phosphorylation of MBP by PAK2. The initial velocities for the phosphorylation of MBP by PAK2 were measured under different viscosogen concentrations. The dominant effect of the viscosogen appears to be on k_{cat} with little or no significant effect on the second-order rate constant, k_{cat}/K_{mB}. The value of k_{cat} decreased from 12 to 3.8 s^{-1} in 40% sucrose. The slope of a plot of k_{cat}^0/k_{cat} versus η^{rel}, $(k_{cat})^\eta$, which indicates the sucrose effect on MBP phosphorylation, was determined to be 0.62 ± 0.02. From these values, the rates of product release and phosphoryl group transfer can then be calculated as $k_4^0 = k_{cat}^0/(k_{cat})^\eta = 19$ s^{-1} and $k_3 = k_{cat}^0/[1 - (k_{cat})^\eta] = 31$ s^{-1}, respectively. The dissociation of products, ADP and phospho-MBP, is combined in k_4^0, and the viscosity method cannot discern which product release step controls k_4^0 without other kinetic experiments. The lack of a viscosity effect on k_{cat}/K_{mB} predicts that the value of k_{-2}^0 is at least 10-fold greater than that of k_3 (i.e., $k_{-2}^0 \geq 306$ s^{-1}. Therefore, the lower limit of the association rate constant of MBP with the PAK2−ATP complex can be estimated as $k_2^0 = (k_{cat}/K_{mB})^0 \times (k_{-2}^0 + k_3)/k_3 \geq 7.5 \times 10^6$ M^{-1} s^{-1}. Moreover, when the concentration of ATP was doubled at the highest relative viscosity, the rate of MBP phosphorylation did not change (data not shown), confirming that under these conditions initial velocity measurements represent true k_{cat} values.

There are two classes of additives that markedly change the viscosity of aqueous solution: (a) monomeric polyhydroxylated molecules such as sucrose or glycerol and (b) polymeric species such as polyacrylamide or ficoll. In general, the addition of polymeric viscosogenic agents affects the measured viscosity of the solution but has no effect on the diffusion behavior of small molecules or on the rates of diffusion-controlled reactions. On the other hand, the addition of small-molecule viscosogens affects both the measured viscosity and the rates of diffusive processes (*42*). To test whether the observed reaction rate changes are due to changes in the macroviscosogenic properties of sucrose, we examined the kinetics of MBP phosphorylation in the presence of a macroviscosogen, Ficoll 400. Such high molecular weight polymers are expected to result in altered macroviscosogenic properties of the solvent without affecting the diffusional rates of small molecules in solution (*44*). We observed no viscosity effect on either k_{cat} or k_{cat}/K_{mB} when Ficoll 400 was the viscosogenic agent (Figure 5). Evidently, the viscosity effects observed using sucrose are due to the altered diffusional rates but not due to changes in the macroviscosogenic properties of this cosolvent.

Saturating MBP and Varying ATP Concentrations. We next tested the effect of increased solvent viscosity on the

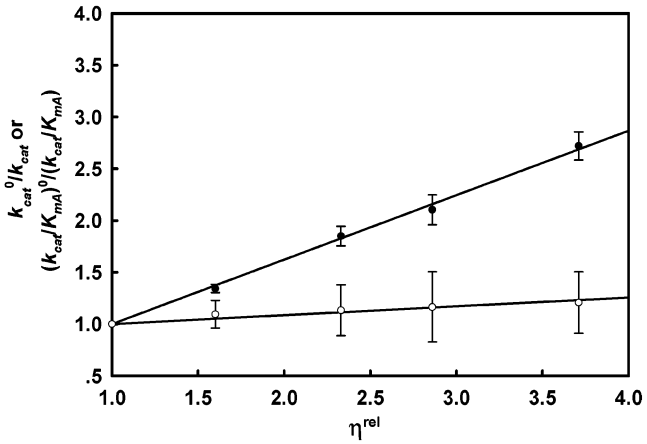

FIGURE 6: Dependence of the steady-state kinetic parameters of the MBP phosphorylation on the relative viscosity of solvent at saturating MBP concentration. η^{rel} represents the ratio of solution viscosity in the presence of sucrose over that in the absence of sucrose. k_{cat}^0/k_{cat} (●) and $(k_{cat}/K_{mA})^0/(k_{cat}/K_{mA})$ (○) are the ratios of the observed k_{cat} and k_{cat}/K_{mA} values in the absence and presence of viscosogen, respectively. The MBP concentration was at 200 μM with varying ATP concentrations.

catalytic reaction mechanism when the concentration of ATP was varied and the amount of MBP was fixed. The effect of increasing solvent viscosity on the steady-state kinetic parameters for the phosphorylation of MBP by PAK2 is shown in Figure 6. At saturating MBP concentration (200 μM), the viscosity effect on k_{cat} was identical within error ($(k_{cat})^\eta = 0.6$) to that observed when the MBP concentration was varied under saturating ATP. Identical results were obtained at 1 mM MBP. By comparison, a small viscosity effect on k_{cat}/K_{mA} at high MBP concentrations was observed ($(k_{cat}/K_{mA})^\eta = 0.09 \pm 0.01$). If an ordered mechanism (with ATP binding first) is assumed, when [B] is very large, eq 3 becomes

$$v = \frac{\dfrac{k_3k_4}{(k_3 + k_4)}[E]_0[A]}{\dfrac{k_3k_4}{k_1(k_3 + k_4)} + [A]} = \frac{k_{cat}[E]_0[A]}{K_{mA} + [A]} \qquad (13)$$

The value for k_{cat}/K_{mA} in such a mechanism would be equal to k_1, and the viscosity effect on the parameter would be predicted as $(k_{cat}/K_{mA})^\eta = 1$ at saturating concentrations of MBP. Our viscosity data, apparently, conflicts with such an ordered binding mechanism. On the other hand, if the mechanism is assumed to be random, under the condition of saturating MBP the mechanism of PAK2-catalyzed MBP phosphorylation can be written as

$$A + EB \underset{k'_{-2}}{\overset{k'_2}{\rightleftharpoons}} EAB \xrightarrow{k_3} EPQ \xrightarrow{k_4} E + P + Q$$

In this scheme, the substrate ATP combines with the enzyme−MBP complex to form the active ternary complex by the second-order association rate constant, k'_2, and the dissociation rate constant, k'_{-2}. The slope of a plot of $(k_{cat}/K_{mA})^0/(k_{cat}/K_{mA})$ versus η^{rel} is given by

$$\left(\frac{k_{cat}}{K_{mA}}\right)^\eta = \frac{k_3}{k'^{\,0}_{-2} + k_3} \qquad (14)$$

Since the value of k_3 is known, from the slope of $(k_{cat}/K_{mA})^0/(k_{cat}/K_{mA})$ versus η^{rel}, $(k_{cat}/K_{mA})^\eta = 0.09$, the dissociation rate constant of ATP from the enzyme−MBP complex can then be estimated as $k'^{\,0}_{-2} = k_3[1 - (k_{cat}/K_{mA})^\eta]/(k_{cat}/K_{mA})^\eta = 330$ s^{-1}. The association rate constant of ATP to the enzyme−MBP complex can be calculated as $k'^{0}_{2} = (k_{cat}/K_{mA})^0(k'^{\,0}_{-2} + k_3)/k_3 = 1.9 \times 10^6$ M^{-1} s^{-1}.

Phosphorylation of LIMKtide. Small synthetic peptides can serve as efficient substrates for a number of protein kinases (*45*, *46*). To study the PAK2-catalyzed reaction in the context of a different substrate, we used a synthetic peptide derived from LIM kinase (LIMKtide) that contains a PAK2 phosphorylation site Thr-508 (*16*). The phosphorylation kinetics of LIMKtide in 0, 25, and 36% sucrose are shown in Figure 7A as a plot of the observed initial rate versus LIMKtide concentration. Typical Michaelis−Menten behavior was observed in the absence and presence of the viscosogen. Figure 7B shows the effect of increasing solvent viscosity on the steady-state kinetic parameters for the phosphorylation of LIMKtide by PAK2. The slope of k_{cat}^0/k_{cat} versus η^{rel} ($(k_{cat})^\eta$), for the sucrose effect on LIMKtide phosphorylation, was determined to be 0.18 ± 0.01. From this value, the rates of product release and phosphoryl group transfer can be estimated as $k_4^0 = k_{cat}^0/(k_{cat})^\eta = 86$ s^{-1} and $k_3 = k_{cat}^0/[1 - (k_{cat})^\eta] = 19$ s^{-1}, respectively (Table 2). The dissociation of products, ADP and phosphorylated peptide, is combined in k_4^0. In the case of protein kinase A, the ADP release rate is rate limiting with respect to substrate processing, and k_4^0 refers to the dissociation rate constant of ADP alone (*47*, *48*). Assuming the same for the PAK-catalyzed reactions, the value of k_4^0 so-determined should be independent of protein substrate species. A comparison of the k_4^0 values in Tables 1 and 2 indicates that k_4^0 for LIMKtide is more than 4-fold larger than that for MBP, suggesting that the release of phospho-MBP product is likely partially rate determining in PAK2 catalysis. Similar to the case of the phosphorylation of MBP, little or no significant effect on the second-order rate constant, k_{cat}/K_{mB}, was observed. Thus, the dissociation rate of LIMKtide must be sufficiently faster than the phosphoryl transfer step. The slope of the plot of $(k_{cat}/K_{mB})^0/(k_{cat}/K_{mB})$ versus η^{rel} was determined to be $(k_{cat}/K_{mB})^\eta = 0.03 \pm 0.01$. From this value, the dissociation and association rate constants of LIMKtide can be calculated as $k_{-2}^0 = k_3[1 - (k_{cat}/K_{mB})^\eta]/(k_{cat}/K_{mB})^\eta = 708$ s^{-1} and $k_2^0 = (k_{cat}/K_{mB})^0(k_{-2}^0 + k_3)/k_3 = 31 \times 10^6$ M^{-1} s^{-1}, respectively (Table 2). Since the dissociation rate of protein substrate from the enzyme is about 10-fold greater than that of phosphoprotein product, the slower release rate of product from the PAK2 active site implies that phosphoprotein binds better than the substrate protein if the phosphorylation of protein substrate does not affect the association rate constant significantly.

GST Pull-Down Assays. To further confirm the random binding mechanism and examine whether GST-PAK2 and MBP interact directly, a pull-down assay was performed in the absence of ATP. The purified GST-PAK2 was activated by autophosphorylation in the presence of constitutively

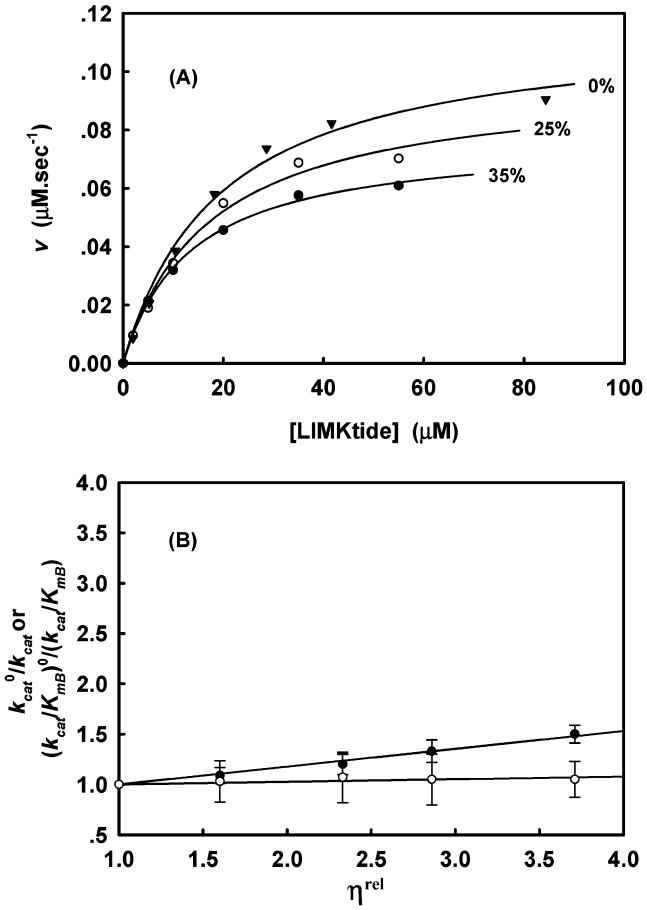

FIGURE 7: Dependence of the steady-state kinetic parameters of the LIMKtide phosphorylation on the relative viscosity of solvent. (A) Plot of initial rate versus LIMKtide concentration in the presence of 0 (▲), 25 (○), and 35% (●) sucrose. The kinase reactions were carried out in a reaction mixture containing the standard assay buffer (pH 7.4), GST-PAK2 (7.5 nM), and the indicated concentrations of LIMKtide at 25 °C. The concentration of ATP was at 1 mM. (B) Solvent viscosity effects on k_{cat} and k_{cat}/K_{mB} for the LIMKtide phosphorylation. The ATP concentration was at 1 mM, and LIMKtide concentration was varied. η^{rel} represents the ratio of solution viscosity in the presence of sucrose over that in the absence of sucrose. k_{cat}^0/k_{cat} (●) and $(k_{cat}/K_{mB})^0/(k_{cat}/K_{mB})$ (○) are the ratios of the observed k_{cat} and k_{cat}/K_mvalues in the absence and presence of viscosogen, respectively. The dashed line has a slope of 1.

active GST-Cdc42L61 as described before. The phosphorylated active GST-PAK2 (~100 μg) was immobilized on glutathione-coupled Sepharose and incubated in protein binding buffer (50 mM Tris, pH 7.4, 100 mM NaCl, 2 mM EDTA) with 400 μg of MBP for 30 min at room temperature. The samples were then washed completely (more than 10 times) with binding buffer and boiled in SDS sample buffer. The GST-PAK2, GST-Cdc42L61, and any associated protein were resolved by SDS−PAGE gel and analyzed by Coomassie Blue staining. The result shows that a complex that contained MBP protein was released from the Sepharose beads (Figure 8). When GST-Cdc42L61 was examined under similar conditions, neither Cdc42L61 nor GST was able to pull down a detectable amount of MBP, indicating that MBP was unable to form the binary complex with Cdc42L61 or GST. Therefore, the immobilized GST-PAK2 fusion protein was shown to bind specifically to MBP in the absence of ATP.

Table 2: Kinetic Constants and Viscosity Effects for Phosphorylation of LIMKtide by PAK2[a]

kinetic parameter	value	method of determination
k_{cat}	$16 \pm 1\ s^{-1}$	measured
$K_{m(LIMKtide)}$	$19 \pm 3\ \mu M$	measured
$(k_{cat})^{\eta}$	0.18 ± 0.01	measured
$(k_{cat}/K_{m(LIMKtide)})^{\eta}$	0.03 ± 0.01	measured
$k_{cat}/K_{m(LIMKtide)}$	$0.8 \pm 0.1\ \mu M^{-1}\ s^{-1}$	$k_{cat}/K_{m(LIMKtide)}$
$k_{2(LIMKtide)}$	$31 \pm 9\ \mu M^{-1}\ s^{-1}$	$(k_{cat}/K_{m(LIMKtide)})$ $(k_{-2(LIMKtide)} + k_3)/k_3$
$k_{-2(LIMKtide)}$	$708 \pm 168\ s^{-1}$	$k_3(1-(k_{cat}/K_{m(LIMKtide)})^{\eta})/$ $(k_{cat}/K_{m(LIMKtide)})^{\eta}$
k_3	$19 \pm 1\ s^{-1}$	$k_{cat}/(1-(k_{cat})^{\eta})$
k_4	$86 \pm 5\ s^{-1}$	$k_{cat}/(k_{cat})^{\eta}$

[a] The kinetic parameters were measured in 50 mM MOPS (pH 7.4) buffer at 25 °C using a coupled enzyme assay. [PAK2] = 7.5 nM, [ATP] = 1 mM, and [LIMKtide] = 2−85 μM, 10 mM $MgCl_2$. k_{cat} and $K_{m(LIMKtide)}$ were directly measured from the steady-state kinetic analysis. $(k_{cat})^{\eta}$ and $(k_{cat}/K_{m(LIMKtide)})^{\eta}$ are the slope values for plots of the steady-state kinetic parameters as ratios in the absence and presence of sucrose versus the relative solvent viscosities.

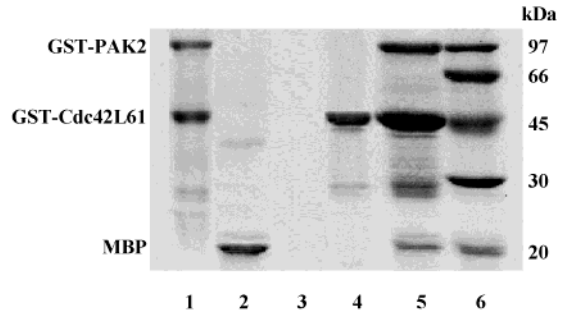

FIGURE 8: Interaction between GST-PAK2 and MBP in the absence of ATP. GST-PAK2 and MBP proteins interact in vitro in a GST pull-down assay. Phosphorylated GST-PAK2 and GST-Cdc42L61 were immobilized on glutathione-coupled Sepharose prior to incubation with MBP (lane 1). The immobilized sample was incubated with MBP for 30 min at room temperature and then washed with binding buffer completely until no MBP was detected in the buffer (lane 3). Bound proteins, released from the Sepharose by boiling in SDS sample buffer, were resolved by 12% SDS−PAGE (lane 5). In a control experiment, immobilized GST-Cdc42L61 was incubated with MBP for 30 min at room temperature. The GST-Cdc42L61 and any associated protein were analyzed by 12% SDS−PAGE after extensive wash (lane 4). The purified MBP ran as a single ~20 kDa band on a 12% SDS−PAGE gel (lane 2). The molecular mass markers of 97, 66, 45, 30, and 20 kDa are indicated on the right (lane 6).

DISCUSSION

Complete Kinetic Scheme of PAK2-Catalyzed Reaction. Since protein phosphorylation reactions involve the participation of ATP in addition to the protein substrate, a number of mechanisms are possible for these two-substrate reactions. A rapid-equilibrium random mechanism was found to be involved in the phosphorylation reaction of rabbit muscle myosin light chain kinase (*49*), while a steady-state kinetic analysis of the EGF receptor tyrosine kinase using a synthetic peptide suggested that catalysis occurs by an ordered reaction. In this model, the peptide substrate binds to the catalytic site first, followed by ATP binding (*50*). In the case of cAMP-dependent protein kinase A (cAPK), there have been some inconsistent reports concerning the kinetic mechanism (*31*, *47*, *48*, *51*−*55*). Whitehouse et al. analyzed the reaction mechanism using MgATP, peptide substrate, substrate analogues, and protein kinase inhibitor and concluded that

the steady-state kinetics of cAPK follows an ordered mechanism in which ATP binds first (*55*). However, Kong and Cook (*47*) and Adams and Taylor (*48*) have shown, definitively using isotope partitioning and viscosity-dependent kinetic experiments, that cAPK conforms to a random kinetic mechanism, and there is a preferred binding order under limiting amounts of peptide with ATP binding first.

As mentioned above, the form of the steady-state rate equations cannot discriminate between the rapid-equilibrium random and ordered ternary-complex mechanism, nor, if the mechanism is an ordered one, can the order of substrate addition be determined on the basis of the equations. Therefore, it is essential to employ alternative procedures for differentiating these mechanisms. Enzyme inhibition studies and isotopic exchange have been successfully used for this purpose before. To access the microscopic rate constants of the partial reactions within the enzymatic mechanism of PAK2, we employed a steady-state solvent viscosometric method, which allows separation of the diffusive from nondiffusive steps. In practice, viscosogens could have nonspecific effects on enzymatic reactions. Such nonspecific effects may be related to changing the structure and/or reactivity of the substrates, enzyme, or other components of reaction media. Interpretation of viscosity effects as diffusional must be based on controlling for these interactions. In our case, the observed viscosity effects on both k_{cat} and k_{cat}/K_m of PAK2-catalyzed reactions can be attributed specifically to the microviscosogenic properties of the cosolvent and not to the solvent macroviscosity for the following reasons: (1) No viscosity effects on the kinetics of MBP phosphorylation were observed in the presence of a macroviscosogen, Ficoll 400. (2) No viscosity effect on the maximal ATPase rate for PAK2 were observed in the presence of sucrose. (3) No viscosity effects in sucrose were observed on k_{cat}/K_m for MBP, suggesting that the decrease in k_{cat} is not a result of substrate competition by sucrose.

The steady-state kinetic data and the effects of solvent viscosity on the phosphorylation of MBP can be combined to outline a complete kinetic mechanism for the PAK2-catalyzed reaction. When a data set of initial reaction velocities obtained under conditions of varying MBP concentrations at several fixed ATP concentrations was analyzed, double reciprocal plots show linearity over a wide range for both MBP and ATP, and intersecting line patterns were observed. The interaction patterns of the reactants were compared with the patterns of frequently observed bisubstrate reaction models described in (*56*). A ping-pong mechanism (where a parallel line pattern is characteristic) can be excluded from such analysis. By examining the effects of increased solvent viscosity on the catalytic reaction mechanism when the concentration of ATP was varied with saturating MBP, a compulsorily ordered bi-bi mechanism can be excluded. Note that the lack of deviation from linearity of double reciprocal plots is consistent with, but not a proof of, a rapid-equilibrium random mechanism. In this mechanism, association and dissociation of both ATP and MBP are fast as compared to the catalysis, and there is no obligate order of binding of the substrates. Further supporting evidences for the rapid-equilibrium random mechanism come from viscosity experiments. Since no significant viscosity effects on k_{cat}/K_m were observed, both ATP and MBP dissociate much faster than the phosphoryl group transfer of ATP to the MBP. (i.e., k_{-2}, $k'_{-2} \gg k_3$). This implies that both substrates are in rapid-equilibrium with PAK2. In addition, the fact that the value of K_{iA} determined from the steady-state kinetics is similar to the dissociation constant between ATP and free PAK2 is also consistent with the rapid-equilibrium random mechanism. The final step in Scheme 1 (k_4) describes the net bimolecular rate constant for the release of both products, and the viscosity measurements cannot distinguish between the dissociation rate constants for the phosphorylated MBP and ADP. Taken together, our data are consistent with the fast random addition of ATP and MBP to the PAK2 active site. The kinetic constants derived for the overall phosphorylation of MBP are shown in Scheme 2.

Scheme 2

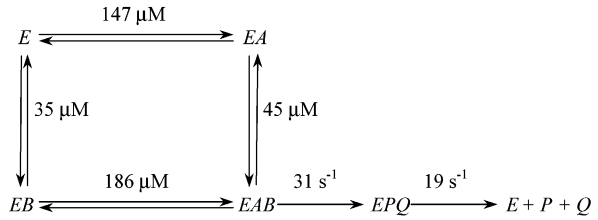

Comparison of PAK2 with Other Serine/Threonine Protein Kinases. The increasing database on protein kinase structures now permits a comparative analysis of their catalytic functions. One of the better-characterized protein kinases is the catalytic subunit of cAMP-dependent protein kinase (cAPK). In the absence of the second messenger, cAMP, cAPK exists in an inactive tetramer composed of two catalytic subunits and a regulatory dimer. The binding of cAMP to the regulatory portion induces a conformational change that leads to the immediate breakdown of the tetramer into its constituent catalytic and regulatory subunits. The catalytic subunit can then bind and phosphorylate protein or peptide substrate in an ATP-dependent manner. Viscosometric studies indicated that the maximal rate constant, k_{cat}, is diffusion limited (i.e., the release of one of the products controls maximum turnover rate). The rate of phosphoryl group transfer is predicted to be at least 10-fold larger than k_{cat} (*48*, *57*).

Another set of well-studied protein kinases are the mitogen-activated protein kinases (MAP kinases). This family of enzymes comprises the ERK, JNK, and p38 protein kinase subfamilies. Among members of the protein kinase superfamily, the MAP kinases display unique biochemical properties in terms of both their mechanism of regulation and also their substrate specificity. While the activation of most, but not all, protein kinases requires the phosphorylation of a single site within a structurally conserved segment termed the activation loop, the MAP kinases are activated by dual-phosphorylation on a conserved threonine phosphorylation site and an additional neighboring tyrosine residue (*58*). Phosphorylation of both residues is essential for full catalytic activity (*59*) and is mediated by a dual-specificity MAP kinase kinase (*60*). Prowse et al. employed steady-state kinetic and solvent viscosometric techniques to characterize the catalytic reaction pathway of the MAP kinase ERK2 with respect to the phosphorylation of MBP and a synthetic peptide substrate, ERKtide (*29*). Extensive mechanistic studies have shown that this enzyme will phosphorylate threonine-containing peptides with a random kinetic mech-

Scheme 3

$$EA + B \underset{k_{-2}}{\overset{k_2}{\rightleftharpoons}} EAB \xrightarrow{k_3} EPQ \xrightarrow{k_4} E + P + Q$$

cAPK	2.3 $\mu M^{-1}s^{-1}$	500 s^{-1}	21 s^{-1}
	(3350 s^{-1})		
ERK2	$\geq$ 2 $\mu M^{-1}s^{-1}$	12 s^{-1}	56 s^{-1}
	($\leq$ 1.2 s^{-1})		
PAK2	$\geq$ 7.5 $\mu M^{-1}s^{-1}$	31 s^{-1}	19 s^{-1}
	($\geq$ 306 s^{-1})		

anism. In contrast to cAPK, the substrate processing occurs via slow phosphoryl group transfer followed by the faster release of products in the case of ERK2.

The data presented herein permits a detailed comparison of the catalytic properties of PAK2 with these kinases by evaluating the individual steps in their respective mechanisms. Scheme 3 lists the rate constants for the phosphorylation of Kemptide and MBP by the catalytic subunit of cAPK, ERK2, and PAK2, respectively.

Two similarities among the three protein kinases are apparent in Scheme 3. The binding rates of the substrate and the net release rates of the products are similar despite that the substrates and products differ in size, charge, and amino acid composition. While ADP release has been shown to be rate limiting in protein kinase A catalysis (*61*), our studies suggest that the release of phospho-MBP product is likely partially rate determining for the PAK2-catalyzed reaction since the dissociation rate of products from the PAK2 active site (k_4) for LIMKtide phosphorylation differs from that of MBP by more than 4-fold. One major difference between the kinetic mechanisms of cAPK and PAK2 lies in the more than 10-fold faster rate of phosphoryl group transfer in cAPK-catalyzed reaction as compared to PAK2. Since the phosphoryl group transfer rate is only 7-fold slower than the dissociation rate of the substrate from the enzyme ($k_{-2}/k_3 = 6.7$), the phosphorylation of Kemptide by cAPK proceeds with near rapid-equilibrium binding of substrate (*48*, *57*). The most unique feature for ERK2 is the dramatically slower dissociation rate of MBP from the ERK2 active site in comparison to the release rate of MBP and Kemptide from the active sites of their respective enzymes, PAK2 and cAPK. The physical basis for the slow dissociation rate of MBP from ERK2 is not clear at present. The observed differences in the individual steps for these three enzymes have only a small effect on the maximal rate constant, k_{cat} (21 s^{-1} in cAPK, 10 s^{-1} in ERK2, and 12 s^{-1} in PAK2) but have a relatively large effect on k_{cat}/K_m. The k_{cat}/K_m value for cAPK is about 3×10^5 M^{-1} s^{-1}, while that for ERK2 is 2.4×10^6 M^{-1} s^{-1}.

In summary, we present a detailed kinetic analysis of recombinant human PAK2 in the current study. We demonstrate that PAK2 employs a rapid-equilibrium random kinetic mechanism in substrate phosphorylation. By steady-state kinetic and solvent viscosometric techniques, we have assigned the rate constant values, or limits thereof, to each step in the overall kinetic scheme for the phosphorylation of MBP and LIMKtide by PAK2. These results allow a direct comparison of the kinetic properties of a PAK family member with that of cAPK and ERK and provide important insight for future structural and mechanistic interpretation of the kinase functions.

REFERENCES

1. Hunter, T. (1987) *Cell 50*, 823−829.
2. Manser, E., Leung, T., Salihuddin, H., Zhao, Z., and Lim, L. (1994) *Nature 363*, 364−367.
3. Daniels, R. H., and Bokoch, G. M. (1999) *Trends Biochem. Sci. 24*, 350−355.
4. Lim, L., Manser, E., Leung, T., and Hall, C. (1996) *Eur. J. Biochem. 242*, 171−185.
5. Sells, M. A., and Chernoff, J. (1997) *Trends Cell Biol. 7*, 162−167.
6. Bagrodia, S., and Cerione, R. A. (1999) *Trends Cell Biol. 9*, 350−355.
7. Brown, J. L., Stowers, L., Baer, M., Trejo, J., Coughlin, S., and Chant, J. (1996) *Curr. Biol. 6*, 598−605.
8. Martin, G. A., Bollag, G., McCormick, F., and Abo, A. (1995) *EMBO J. 14*, 1970−1978.
9. Bagrodia, S., Taylor, S. J., Creasy, C. L., Chernoff, J., and Cerione, R. A. (1995) *J. Biol. Chem. 270*, 22731−22737.
10. Abo, A., Qu, J., Cammarano, M. S., Dan, C., Fritsch, A., Baud, V., Belisle, B., and Minden, A. (1998) *EMBO J. 17*, 6527−6540.
11. Dan, C., Nath, N., Liberto, M., and Minden, A. (2002) *Mol. Cell. Biol. 22*, 567−577.
12. Lee, S. R., Ramos, S. M., Ko, A., Masiello, D., Swanson, K. D., Liu, M. L., and Balk, S. P. (2002) *Mol. Endocrinol. 16*, 85−99.
13. Knaus, U. G., and Bokoch, G. M. (1998) *Int. J. Biochem. Cell Biol. 30*, 857−862.
14. Sells, M. A., Knaus, U. G., Bagrodia, S., Ambrose, D. M., Bokoch, G. M., and Chernoff, J. (1997) *Curr. Biol. 7*, 202−210.
15. Sanders, L. C., Matsumura, F., Bokoch, G. M., and de Lanerolle, P. (1999) *Science 283*, 2083−2085.
16. Edwards, D. C., Sanders, L. C., Bokoch, G. M., and Gill, G. N. (1999) *Nat. Cell Biol. 1*, 253−259.
17. Polverino, A., Frost, J., Yang, P., Hutchison, M., Neiman, A. M., Cobb, M. H., and Marcus, S. (1995) *J. Biol. Chem. 270*, 26067−26070.
18. Zhang, S., Han, J., Sells, M. A., Chernoff, J., Knaus, U. G., Ulevitch, R. J., and Bokoch, G. M. (1995) *J. Biol. Chem. 270*, 23934−23936.
19. Bagrodia, S., Derijard, B., Davis, R. J., and Cerione, R. A. (1995) *J. Biol. Chem. 270*, 27995−27998.
20. Sun, H., King, A. J., Diaz, H. B., Marshall, M. S. (2000) *Curr. Biol. 10*, 281−284.
21. Frost, J. A., Steen, H., Shapiro, P., Lewis, T., Ahn, N., Shaw, P. E., and Cobb, M. H. (1997) *EMBO J. 16*, 6426−6438.
22. Downward, J. (1999) *Nat. Cell Biol. 1*, E33−E35.
23. Schurmann, A., Mooney, A. F., Sanders, L. C., Sells, M. A., Wang, H. G., Reed, J. C., and Bokoch, G. M. (2000) *Mol. Cell Biol. 20*, 453−461.
24. Tang, Y., Zhou, H., Chen, A., Pittman, R. N., and Field, J. (2000) *J. Biol. Chem. 275*, 9106−9109.
25. Rudel, T., and Bokoch, G. B. (1997) *Science 276*, 1571−1574.
26. Rudel, T., Zenke, F. T., Chuang, T. H., and Bokoch, G. M. (1998) *J. Immunol. 160*, 7−11.
27. Bokoch, G. M. (1998) *Cell. Death Differ. 5*, 637−645.
28. Knaus, U. G., Morris, S., Dong, H. J., Chernoff, J., and Bokoch, G. M. (1995) *Science 269*, 221−223.
29. Prowse, C. N., Hagopian, J. C., Cobb, M. H., Ahn, N. G., and Lew, J. (2000) *Biochemistry 39*, 6258−6266.
30. Gill, S. C., and von Hippel, P. H. (1982) *Anal. Biochem. 182*, 319−326.
31. Cook, P. F., Neville, M. E., Jr., Vrana, K. E., Hartl, F. T., and Roskoski, R., Jr. (1982) *Biochemistry 21*, 5794−5799.
32. Shoemaker, D. P., and Carland, C. W. (1962) *Experiments in Physical Chemistry*, 2nd ed., McGraw-Hill, New York.
33. Freifelder, D. (1982) *Physical Biochemistry: Applications to Biochemistry and Molecular Biology*, 2nd ed., W. H. Freeman and Co., New York.
34. Gatti, A., Huang, Z., Tuazon, P. T., and Traugh, J. A. (1999) *J. Biol. Chem. 274*, 8022−8028.
35. Lei, M., Lu, W., Meng, W., Parrini, M. C., Eck, M. J., Mayer, B. J., and Harrison, S. C. (2000) *Cell 102*, 387−397.

36. Tuazon, P. T., Spanos, W. C., Gump, E. L., Monnig, C. A., and Traugh, J. A. (1997) *Biochemistry 36*, 16059−16064.
37. Laidler, K. J., and Bunting, P. S. (1973) *The Chemical Kinetics of Enzyme Action*, 2nd ed., pp 119−125, Oxford University Press, Oxford.
38. Seubert, F. A., Renosto, F., Knudson, P., and Segel, I. H. (1985) *Arch. Biochem. Biophys. 240*, 509−523.
39. Caldin, E. F. (1964) *Fast Reaction in Solution*, Wiley, New York.
40. Nakatani, H., and Dunford, H. B. (1979) *J. Phys. Chem. 83*, 2662−2665.
41. Brouwer, A. C., and Kirsch, J. F. (1982) *Biochemistry 21*, 1302−1307.
42. Blacklow, S. C., Raines, R. T., Lim, W. A., Zamore, P. D., and Knowles, J. R. (1988) *Biochemistry 27*, 1158−1167.
43. Cleland, W. W. (1975) *Biochemistry 14*, 3220−3224.
44. Phillips, H. O., Marcinkowsky, A. I., Sachs, S. B., and Kraus, K. A. (1977) *J. Phys. Chem. 81*, 679−682.
45. Kemp, B. E., and Pearson, R. B. (1990) *Trends Biochem. Sci. 15*, 342−346.
46. Kemp, B. E., Parker, M. W., Hu, S., Tiganis, T., and House, C. (1994) *Trends Biochem. Sci. 19*, 440−444.
47. Kong, C. T., and Cook, P. F. (1988) *Biochemistry 27*, 4795−4799.
48. Adams, J. A., and Taylor, S. S. (1992) *Biochemistry 31*, 8515−8522.
49. Geuss, U., Mayr, G. W., and Heilmeyer, L. M. G. (1985) *Eur. J. Biochem. 153*, 327−334.
50. Erneux, C., Cohen, S., and Garbers, D. L. (1983) *J. Biol. Chem. 258*, 4137−4142.
51. Moll, G. W., Jr., and Kaiser, E. T. (1976) *J. Biol. Chem. 251*, 3993−4000.
52. Matsuo, M., Chang, L., Huang, C., and Villar-Palasi, C. (1978) *FEBS Lett. 87*, 77−79.
53. Pomerantz, A. H., Allfrey, V. G., Merrifield, R. B., and Johnson, E. M. (1977) *Proc. Natl. Acad. Sci. U.S.A. 74*, 4261−4265.
54. Kochetkov, S. N., Bulargina, T. V., Sashchenko, L. P., and Severin, E. S. (1977) *Eur. J. Biochem. 81*, 111−118.
55. Whitehouse, S., Feramisco, J. R., Casnellie, J. E., Krebs, E. G., and Walsh, D. A. (1983) *J. Biol. Chem. 258*, 3693−3701.
56. Segel, I. H. (1975) *Enzyme Kinetics*, Wiley-Interscience, New York.
57. Grant, B. D., and Adams, J. A. (1996) *Biochemistry 35*, 2022−2029.
58. Cobb, M. H., and Goldsmith, E. J. (1995) *J. Biol. Chem. 270*, 14843−14846.
59. Robinson, M. J., Cheng, M., Khokhlatchev, A., Ebert, D., Ahn, N., Guan, K. L., Stein, B., Goldsmith, E., and Cobb, M. H. (1996)- *J. Biol. Chem. 271*, 29734−29739.
60. Ahn, N. G., Seger, R., and Krebs, E. G. (1992) *Curr. Opin. Cell Biol. 4*, 992−999.
61. Zhou, J., and Adams, J. A. (1997) *Biochemistry 36*, 15733−15738.

BI026857L